Avrupa Bilim ve Teknoloji Dergisi
Özel Sayı, S. 91-100, Eylül 2020

Araştırma Makalesi

www.ejosat.com ISSN:2148-2683

European Journal of Science and Technology
Special Issue, pp. 91-100, September 2020

Research Article

Modeling of Biosorption of Arsenic (V) On Waste Orange Peel Derived Graphene-Like Porous Carbon by Artificial Neural Network Approach

Ceren Karaman[1]

[1]Akdeniz University, Vocational School of Technical Sciences, Department of Electricity and Energy, Antalya, Turkey. (ORCID: 0000-0001-9148-7253)

(1st International Conference on Computer, Electrical and Electronic Sciences ICCEES 2020 – 8-10 October 2020)

(**DOI:** 10.31590/ejosat.803101)

ATIF/REFERENCE: Karaman, C. (2020). Modeling of Biosorption of Arsenic (V) On Waste Orange Peel Derived Graphene-Like Porous Carbon by Artificial Neural Network Approach. *European Journal of Science and Technology*, (Special Issue), 91-100.

Abstract

The main threats from heavy metals specifically arsenic-contaminated drinking water have been emerging as an environmental and social crucial issue. Herein, the arsenic (V) (As(V)) biosorption performance of waste orange peel (OP) driven-graphene-like porous carbon (GPC) was investigated experimentally and an artificial neural network (ANN) approach was used to model the biosorption process. The initial pH (2.0, 3.0, 4.0, 5.0, 6.0, 7.0, 8.0, and 10.0), initial As(V) concentration (25.0, 50.0, 100.0, 250.0, 500.0 and 750.0 $mg.L^{-1}$), biosorbent dosage (1.0, 2.0, 3.0, 4.0 and 5.0 $g.L^{-1}$), and contact time (0– 120.0 min) were investigated to optimize the biosorption process. The as-synthesized GPC biosorbents with a high specific surface area (985 $m^2.g^{-1}$) and pore volume (1.04 $cm^3.g^{-1}$) offered superior removal efficiency as 88.2% (equilibrium uptake capacity of 46.5 $mg.g^{-1}$) at initial pH 6.0, initial As(V) concentration 100 $mg.L^{-1}$, and biosorbent dosage 2.0 $g.L^{-1}$. A three-layer ANN model was developed to forecast the Ar(V) biosorption performance of GPCs. Several experimental data points were considered as test data to validate the ANN model. The ANN model was performed with the Levengberg-Marquardt algorithm (LMA), linear transfer function (purelin) at the output layer, and a tangent sigmoid transfer function (tansig) in the hidden layer with 12 neurons. The values of coefficient of determination and mean squared error were calculated to be 0.9858 and 0.0014, respectively. The results revealed that the experimental data were in accordance with ANN-driven data as well as reveling the high accuracy of the ANN approach in estimating the target variable. The developed ANN model is useful for the optimization of process conditions for pilot-scale utilization of As(V) biosorption process by GPC.

Keywords: Agricultural Waste, Arsenic(V) removal, Artificial Neural Network (ANN), Biosorption, Modeling, Orange Peel

Yapay Sinir Ağı Yaklaşımı ile Atık Portakal Kabuğundan Elde Edilen Grafen Benzeri Gözenekli Karbon Üzerinde Arsenik (V) Biyosorpsiyonunun Modellenmesi

Öz

Özellikle arsenikle kirlenmiş içme suyundan kaynaklanan ana tehditler, çevresel ve sosyal olarak önemli bir sorun olarak ortaya çıkmaktadır. Burada, atık portakal kabuğundan (OP) üretilmiş grafen benzeri gözenekli karbonun (GPC) arsenik (V) (As (V)) biyosorpsiyon performansı deneysel olarak incelenmiş ve biyosorpsiyon prosesini modellemek için yapay bir sinir ağı (YSA) yaklaşımı kullanılmıştır. Biyosorpsiyon prosesini optimize etmek için başlangıç pH'ı (2.0, 3.0, 4.0, 5.0, 6.0, 7.0, 8.0, 10.0), başlangıç As (V) konsantrasyonu (5.0, 25.0, 50.0, 100.0, 250.0, 500.0 ve 750.0 $mg.L^{-1}$), biyosorbent dozu (1.0, 2.0, 3.0, 4.0 and 5.0 $g.L^{-1}$) ve temas süresi (0– 120.0 dakika) parametreleri incelenmiştir. Yüksek spesifik yüzey alanine (985 $m^2.g$-^{1}) ve gözenek hacmine (1.04 $cm^3.g^{-1}$) sahip GPC biyosorbentleri, 6.0 başlangıç pH değerinde, 2.0 g.L-1 biyosorbent dozunda ve 100 $mg.L^{-1}$ başlangıç As(V) konsantrasyonunda, % 88.2 giderim verimi (denge biyosorpsiyon kapasitesi; 46.5 $mg.g^{-1}$) ile üstün biyosorpsiyon kapasitesi göstermişlerdir. Bu çalışmada,

[1] Corresponding Author: Akdeniz University, Vocational School of Technical Sciences, Department of Electricity and Energy, Antalya, Turkey. (ORCID: 0000-0001-9148-7253), cerenkaraman@akdeniz.edu.tr

GPC'lerin Ar (V) biyosorpsiyon performansının modellemesinde üç katmanlı bir YSA modeli geliştirilmiştir. YSA modelini doğrulamak için elde edilen deneysel veriler, YSA modelinde test verileri olarak kullanıldı. YSA modeli, Levengberg-Marquardt (LMA) algoritması, çıktı katmanında lineer transfer fonksiyonu (purelin) ve 12 nöronlu gizli katmanda tanjant sigma transfer fonksiyonu (tansig) ile gerçekleştirildi. Sonuçlar, deneysel verilerin YSA temelli verilerle uyum içerisinde olduğunu ve YSA yaklaşımının hedef değişkeni tahmin etmedeki yüksek doğruluğunu ortaya koydu. Geliştirilen YSA modeli, GPC tarafından As (V) biyosorpsiyon işleminin pilot ölçekli kullanımı için işlem koşullarının optimizasyonu için yararlıdır.

Anahtar Kelimeler: Tarımsal Atık, Arsenik(V) giderimi, Yapay Sinir Ağları, Biyosorpsiyon, Modelleme, Portakal Kabuğu.

1. Introduction

Arsenic has been recognized as one of the most hazardous mettaloid being part of earth crust and leads to water resources contamination (Irem et al., 2017). Drinking water contamination by arsenic is a crucial issue due to its toxic nature causing cancer or other chronic diseases (Chattopadhyay et al., 2020). Arsenic can be found in natural water as arsenite (As(III)) and arsenate (As(V)). While As(V) are stable in oxygen-rich aerobic environments, As(III) predominate in reducing anaerobic environments such as deep groundwater (Khaskheli et al., 2011). World Health Organization (WHO) has reported arsenic due to its superb toxicity as a Class-I toxicant and set the permissible limit of 10 ppb in drinking water (WHO, 2011). Hence, it is crucial to provide the use of safe drinking water and to meet the water quality standards by developing a new treatment system that can effectively remove the arsenic from aqueous media. In addition to conventional technologies (like coagulation, flocculation, precipitation, ozonation, ion exchange, membrane filtration, etc.) to contribute to the total solution of this problem, several treatment technologies have gained prominences, such as membrane processes, electrochemical techniques, photocatalytic oxidation/degradation, adsorption and combined methods (Kodal and Aksu, 2017, Omwene et al., 2019). Amongst them, adsorption processes have gained prominence since they have high removal efficiency and can be scaled-up (Almasri et al., 2018). Although there are various types of biosorbents, it is important to develop novel biosorbents produced from natural sources or wastes. So far, there have been plenty of studies that have investigated alternative cost-effective and eco-friendly biosorbents. Most recently, agricultural wastes such as waste tea (Çelebi, 2020), coconut shell (Chandana et al., 2020), shrimp shells (He et al., 2020), fungal biomass (Rozman et al., 2020), cherry stones (Ebrahimi et al., 2019), sugar cane bagasse (Guo et al., 2020), coffee bean husk (Tran et al., 2020), rice husk (Ma et al., 2019), etc. have been considered as the most promising candidate for an alternative low-cost, non-toxic, and efficient biosorbents. Owing not only to its high content of different functional groups, such as carboxyl and hydroxyl groups but also to its lignocellulosic content such as of lignin, cellulose, hemicellulose, pectin, etc., waste orange peels can also be used as a satisfactory biosorbent (Liang et al., 2009; Lu et al., 2009; Pathak et al., 2016).
In biosorption process, more experiments mean more precious knowledge on the fundamental understanding of the process. However, in practice, such number of the experimental evaluations are not always possible. Hence, in particular, for large-scale applications, it is important to develop a smart tool for comprehending and forecasting the adsorption capacities of the biosorbents without conducting redundant experiments. Recently, Smart models including random forest (RF), adaptive Neuro-fuzzy inference system (ANFIS), least squares support vector machines (LS-SVM), and artificial neural network have received extensive attention thanks to their unique features (Ghaedi et al, 2014a; Ghaedi et al, 2014b; Nia et al., 2014; Asfaram et al., 2016). Amongst them, ANN is a modeling method that computes the input values by some internal mathematical functions for both linear and non-linear systems to obtain the output values. The capability of approximation arbitrarily complex correlations without exhaustive knowledge of the process is the unique feature of the ANN model (Aghav et al., 2011). In chemical engineering, ANN as a state-of-art tool has also been successfully utilized for modeling of the adsorption equilibrium of solid-liquid systems (Dutta et al., 2010; Elemen et al., 2012), besides former uses such as prediction of activity coefficients of aromatic compounds (Chow et al., 1995), modeling of kinetics of catalytic hydrogenation reaction (Molga et al., 1997), and solubility of proteins (Naik et al., 2005). The performance of the developed ANN model strongly depends on variables such as the number of hidden layers and output layer, the nature of the transfer function, etc. Hence, it is crucial to determine each variable logically. Thanks to its interconnected nature composed of nodes (neurons) and connections (weights), it is possible to obtain complex relationships between independent and dependent variables (Beale et al., 2012).

Bearing all in mind, in this study, it was aimed to develop a cost-natural and locally available biosorbent for As(V) removal from drinking water. Although there has been numerous of investigation about the utilization of orange peel driven adsorbents/biosorbents for removal of heavy metal ions, as far as we know, this work is unique as it is the first time the modeling of biosorption of As(V) onto orange peel-driven biosorbents by using the artificial neural network model. In this work, the three-layer ANN model, which consists of an input layer, hidden layer, and output layer, with an LMA algorithm in MATLAB environment has been used for the estimation of arsenate removal efficiency of GPC. The effect of initial pH, biosorbent dosage ($g.L^{-1}$), initial arsenate concentration ($mg.L^{-1}$), and the contact time (min) on As(V) removal efficiency have been examined in a batch adsorption system and optimum experimental conditions have been ascertained. Subsequently, these experimental data set have been used for the training of the ANN model. The input parameters used for training of the ANN are initial pH, contact time (min), initial As(V) concentration ($mg.L^{-1}$), and biosorbent dosage ($g.L^{-1}$) whereas the removal efficiency of As(V) has been considered as an output of the model. The minimum squared error (MSE) and the determination coefficient have been calculated for forecasting the arsenate removal using the testing data set. The results have indicated there is good accordance between the experimental data and ANN-driven data. The simulations based on the developed ANN model have verified that the ANN model can successfully forecast the biosorption behavior of the As(V) removal under different conditions.

2. Material and Method

2.1. Preparation of Arsenate Solution

Arsenate solutions with initial As(V) concentration range between 25-750 $mg.L^{-1}$ were obtained by diluting the 1000 $mg.L^{-1}$ stock solution of As(V) prepared by sodium arsenate ($Na_2HAsO_4.7H_2O$). The initial pH (ranged between 2.0-10.0) of As(V) solutions were set by using 0.1 N HCl and 0.1 N NaOH solution before introducing the biosorbent.

2.2. Biosorbent Preparation

The waste orange peels were obtained from the BELSO fruit juice production facility Ankara, Turkey, and they were washed with a large volume of tap water, followed by deionized (DI) water. Afterward, they dried in a vacuum oven at 70 °C for 24 h. After ball milling, the biosorbents with lower than *ca*. 300 µm particle size were stored in airtight containers ready for further uses and labeled as dried orange peel (DOP).

GPCs were synthesized from waste orange peel by a two-step synthesis route consisting of thermal annealing and chemical activation. Firstly, the DOP was carbonized at 400 °C under inert nitrogen (N_2) atmosphere for 2 h in a tubular furnace. Subsequently, the as-carbonized DOP powder was mixed with KOH at a mass ratio of 1:2 followed by thermal annealing at 850 °C for 2 h under inert N_2 atmosphere. The obtained product was washed with 0.1 M hydrochloric acid (HCl) and DI water repeatedly until neutral pH to remove inorganic salts. Subsequently, the product was dried at a vacuum oven 70 °C for 24 h, and labeled as graphene-like porous carbon (GPC), stored in a desiccator until use.

2.3. Physicochemical Characterization of Biosorbent

The surface morphologies of samples were characterized by field-emission scanning electron microscope(FE-SEM) (Hitachi S-4900) operating at 5.0 kV, and transmission electron microscope (TEM, JEM-1400F, JEOL) at 120 kV. The Brunauer–Emmett–Teller (BET) surface areas of samples were calculated by the N_2 adsorption/desorption measurements (at 77 K) were performed by Quantachrome Nova 2200 automated surface area analyzer (Quantachrome Corporation, USA) whereas the pore size distributions (PSD) were measured adopting the Barrett-Joyner-Halenda (BJH) method.

2.4. Batch Biosorption Studies

Biosorption studies were conducted by a typical batch process in an Erlenmeyer flask (250 mL) containing 100 mL of arsenate solution. The test samples were agitated in an incubator at a shaking rate of 100 rpm at room temperature of 25 ± 2 °C. The initial pH of the test solution, biosorbent dosage, initial As(V) concentration, and contact time were investigated for their effects on the removal of arsenate. The ranges of investigated biosorption operating condition variables were presented in Table 1.

For biosorption studies, a certain amount of GPC (Table 1.) was added to 100 mL of pH-adjusted As(V) test solution, and this moment was noted as t_0. Afterward, at pre-determined contact time intervals (Table 1), periodically 5.0 mL of arsenate bearing suspensions were taken from the biosorption system and centrifugated at 4000 rpm for 10 min. The remaining As(V) concentration was determined by the atomic absorption spectrometer (AAS) with a flow injection system.

Table 1. Range of biosorbtion operating condition variables

Operating condition variable	Range
Initial pH of the test solution	2.0, 3.0, 4.0, 5.0, 6.0, 7.0, 8.0, 10.0
Initial As(V) concentration ($mg.L^{-1}$)	25.0, 50.0, 100.0, 250.0, 500.0, 750.0
Biosorbent dosage ($g.L^{-1}$)	1.0, 2.0, 3.0, 4.0 5.0
Contact time (min)	0, 1, 2, 3, 4, 5, 10, 15, 20, 25, 30, 35, 40, 45, 50, 60, 90, 120

2.4.1. Evalutaion of Biosorption Performance of GPC

The biosorption capacity q (mg.g^{-1}) (Eq. 1), and removal efficiency % (Eq. 2) values of the GPC were calculated from the arsenate concentrations in water before and after biosorption. All the biosorption experiments were conducted triple to verify the repeatability and accuracy, and the average of them was used for further calculations.

$$q = \frac{(C_0 - C)}{X} \quad (1)$$

$$\text{removal efficiency } \% = \frac{(C_0 - C)}{C_0} \times 100 \quad (2)$$

Where C_o (mg.L^{-1}) is the initial arsenate concentration; C (mg.L^{-1}) is the residual arsenate concentration at any time of the biosorption process; X is the biosorbent dosage (g.L^{-1}); t is the time (min).

2.4.2. Effect of Initial pH

The effect of initial pH of the test solution ranging between 2.0 and 10.0 (Table 1) on the biosorption of As(V) ion was investigated while the other experimental operating condition variables were maintained constant at initial As(V) concentration of 100.0 mg.L^{-1}, biosorbent dosage of 1.0 g.L^{-1}, and contact time 120 min.

2.4.3. Effect of Initial As(V) Concentration

The effect of initial arsenate concentration ranging between 25.0 mg.L^{-1} and 750.0 mg.L^{-1} (Table 1) on the biosorption of As(V) ion was studied at the initial pH of 6.0, biosorbent dosage of 1.0 g.L^{-1}, and contact time over 120 min.

2.4.4. Effect of Contact Time

The effect of contact time was investigated from 0 min to 120 min for initial As(V) concentration range of 25.0 to 750.0 mg.L^{-1} at pH 6.0, and biosorbent dosage of 1.0 g.L^{-1}.

2.4.5. Effect of Biosorbent Dosage

The influence of biosorbent dosage changing between 1.0 -5.0 g.L^{-1} (Table 1) on the removal of As(V) was examined at initial pH of 6.0, initial As(V) concentration of 100.0 mg.mL^{-1}, and the contact time of 120 min.

2.4. Artificial Neural Network Modeling

The three-layer ANN model (Figure 1.), with a tangent sigmoid transfer function (tansig) in the hidden layer, a linear transfer function (purelin) at the output layer and a backpropagation learning algorithm based on the Levenberg-Marquardt algorithm with 1000 iterations was used to forecast the biosorption performance by using the neural network toolbox of MATLAB 9.5 (R2018b) software. The experimental data were grouped randomly into two groups as follows training data set (75 %) and testing data set (25 %). Four neurons including initial pH, initial As(V) concentration (mg.L^{-1}), biosorbent dosage (g.L^{-1}), and contact time (min), 1-20 neurons in the hidden layer, and one neuron (removal %) in the output layer were used. The neurons of each layer are interconnected with weights, in which each processing element is multiplied by its corresponding weight factor, and then added to a neuron's internal threshold (named bias) (Figure 1.). The net input passed through linear/non-linear transfer functions to produce a single output of the neuron (Mustafa et al., 2014; Fawzy et al., 2018). All the data were normalized in the range of 0-1 to prevent numerical overflows due to a very large of small weights.

The performance of the ANN model was evaluated by the minimum mean squared error (MSE) (Eq.3), and the coefficient of determination (R^2) (Eq.4) between the predicted output and the actual target.

$$MSE = \frac{1}{N}\sum_{i=1}^{N}\left(\left|y_{prd,i} - y_{exp,i}\right|\right)^2 \quad (3)$$

$$R^2 = 1 - \frac{\sum_{i=1}^{N}(y_{prd,i} - y_{exp,i})}{\sum_{i=1}^{N}(y_{prd,i} - y_M)} \quad (4)$$

where $y_{prd,i}$ is the predicted value by ANN model, $y_{exp,i}$ is the experimental value, y_M is the average of experimental value, and N is the number of data.

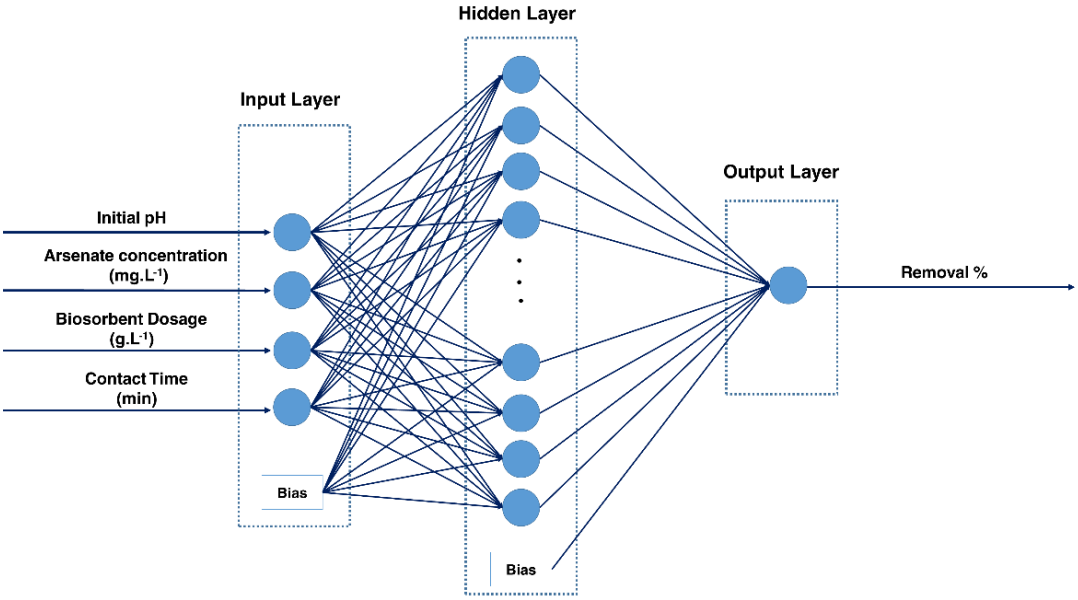

Figure 1. Structure of developed artificial neural network model

3. Results and Discussion

3.1. Physicochemical Characterization of Biosorbent

The morphologies of as-prepared samples were investigated by the SEM and TEM analysis (Figure 2). Although DOP (Figure 2a) presented irregular shape bulk-like carbon monoliths with a relatively smooth surface, GPC (Figure 2b) exhibited a graphene-like silky porous network abundant micro and mesoporous structure. The low-resolution TEM image of GPC (Figure 2c) proved that porous structure and graphitized DOP into the atomic-thick layered carbonaceous material. The TEM image of GPC revealed the fluffy graphene-like structure due to bundles of crumple.

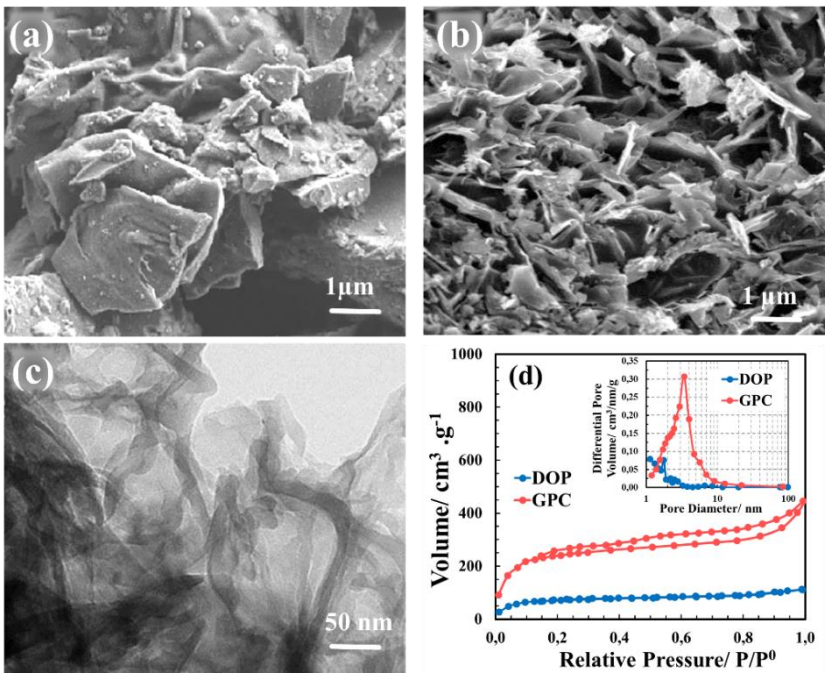

Figure 2. FE-SEM images of (a) DOP and (b) GPC, (c)TEM image of GPC, (d) N_2 adsorption/desorption isotherms (inset the BJH pore size distributions) of DOP and GPC

The porous structures of the DOP and GPC were analyzed by the N_2 adsorption/desorption isotherms (Figure 2d). While DOP presented essentially a Type-I isotherm which confirms the presence of dominant microporous structure (Meng et al., 2017), GPC exhibited type-IV isotherm with an H4 type hysteresis loop (Karaman et al., 2020). The pore size distribution curves (inset of Figure 2d) verified both the microporous structure of DOP and micro and mesoporous structure of GPC. As presented in Table 2, the specific BET surface area

(S_{BET}) of GPC (985 $m^2.g^{-1}$) was almost 8-9 times higher than that of DOP (102.0 $m^2.g^{-1}$). Additionally, the well-ordered pore structure and the large pore volume (1.04 $cm^3.g^{-1}$) of GPC was predicted to favor the biosorption of As (V).

Table 2. Physicochemical parameters obtained from N_2 adsorption/desorption isotherms of DOP and GPC samples

Sample ID	S_{BET} $m^2.g^{-1}$	V_{micro} $cm^3.g^{-1}$	V_{meso} $cm^3.g^{-1}$	V_{total} $cm^3.g^{-1}$	V_{micro} %	V_{meso} %
DOP	102.0	0.10	0.05	0.14	67.38	32.62
GPC	985.0	0.41	0.63	1.04	39.85	60.15

3.2. Batch Biosorption Studies

3.2.1. Effect of Initial pH

The solution pH can affect the protonation of surface functional groups besides the dissociation of the molecules (Das et al., 2007; Su et al., 2010). The pH dependence of the biosorption capacity of GPC was investigated between the pH range out from 2.0 to 10.0 at 100.0 $mg.L^{-1}$ initial As(V) concentration, biosorbent dosage of 1.0 $g.L^{-1}$ over 120 min of contact time. The highest removal capacity of GPC was obtained at pH 6.0 as *ca.* 71.5 $mg.g^{-1}$ (Figure 3). In alkaline media (pH > 7.0), the As(V) biosorption capacity of the GPC decreased since there was probably a competition between the –OH ions and As(V) oxyanions for active sites (Abid et al., 2016; Rahaman et al., 2008). On contrary, at neutral pH values, it could be put forth that there would not be a competition between the –OH or carbonyl groups with the arsenate ions. Hence, it was suggested that the biosorption or As(V) on to GPC probably result in electrostatic interaction between and ion-exchange or complexation between biosorbent and As(V).

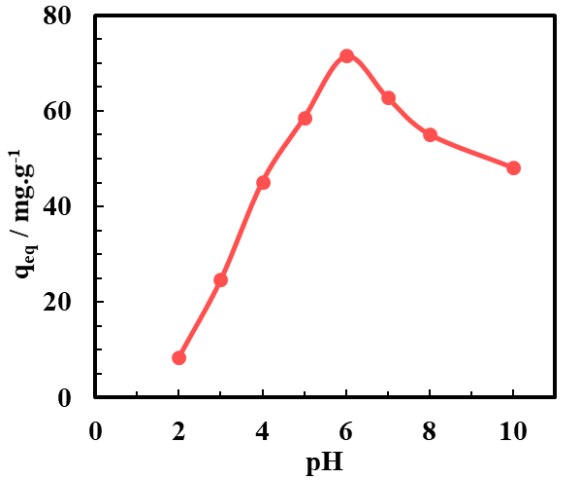

Figure 3. Effect of the initial pH on the equilibrium uptake of As(V) (C_o=100 $mg.L^{-1}$, X=1.0 $g.L^{-1}$; t=120 min).

3.2.2. Effect of Initial As(V) Concentration and Contact Time

The biosorption behavior of GPC was monitored for initial As(V) concentration ranging from 25.0 to 750 $mg.L^{-1}$ at optimum pH of 6.0 and over 120 min contact time. The biosorption behavior of GPC depending on the initial As(V) concentration and contact time was depicted in Figure 4. Biosorption on GPC was enhanced significantly by increasing the initial As(V) concentration tending to saturation at higher concentrations. The equilibrium time of the biosorbent is important to design a cheap and effective biosorption system. Figure 4a exhibited the effect of contact time on biosorption level over 120 min. At the beginning of the biosorption process, the uptake capacity of the biosorbent increased with the contact time linearly and sharply due to more vacant active sites leading to an acceleration of mass transfer of As(V) ions. Then, around 20 min the biosorption curve reached a plateau. It was realized that the majority of As(V) biosorption (*ca.* 80-90 %) on GPC took place within the first 20 min of the whole process and at the end, the biosorbent achieved saturation called equilibrium (q_{eq}). Thanks to its high specific surface area, number of active sites, and the total pore volume and highly-ordered pore size distribution GPC presented high removal efficiency of As(V). Increasing the As(V) concentration provided a considerable driving force to eliminate the effect of mass transfer resistances of the As(V) between solid-liquid interfaces. Moreover, the number of interactions between the biosorbent and the biosorbate relatively increased by the initial As(V) concentration, which boosted the removal capacity of the biosorbent. However, increasing the As(V) concentration diminished the removal efficiency (%) since the active sites of the biosorbent became almost filled (Figure 4b).

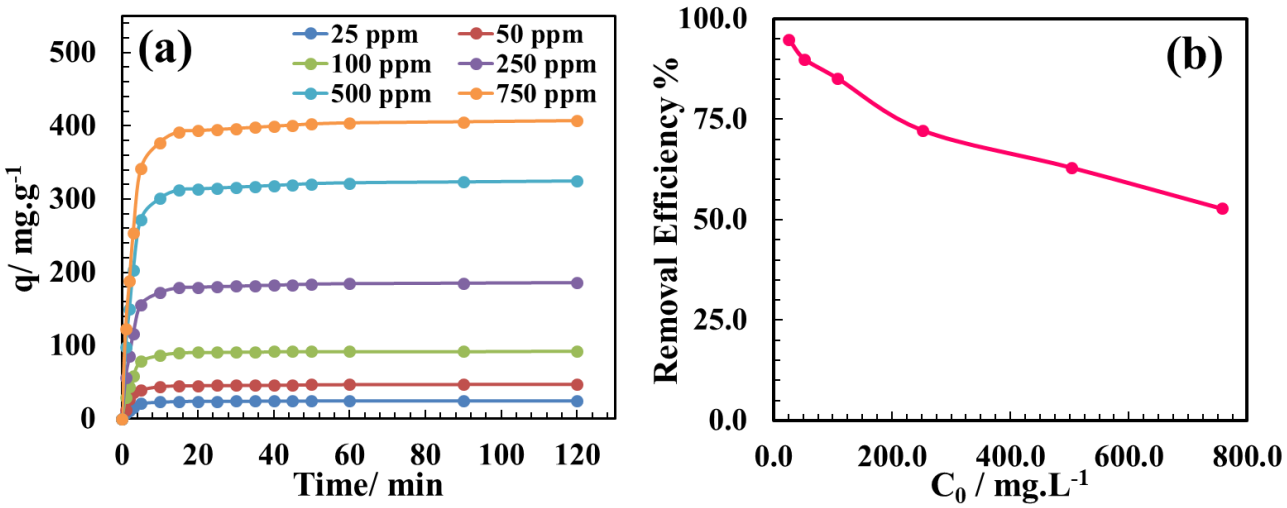

Figure 4. (a)Effects of contact time (min) (b) Effects of initial As(V) concentration (C_0; mg.L^{-1}(ppm) on uptake of As(V)(initial pH=6.0, X=1.0 g.L^{-1})

3.2.3. Effect of Biosorbent Dosage

The effect of biosorbent dosage on As(V) removal was investigated at pH 6.0 over 120 min for 100 mg.L^{-1} initial As(V) concentration. Figure 5. demonstrated that the biosorbent mass fraction directly affected the As(V) removal. It was found that the removal efficiency was increased rapidly from 85.2% to 90.4 % with an increasing amount of biosorbent till 5.0 g.L-1 thanks to the high number of available vacant active sites. Hence, both the diffusion of As(V) ions to the surface of biosorbent and the removal percentage of As(V) was enhanced. However, there was not a significant difference in removal efficiency between 2.0 g.L^{-1} and 5.0 g.L^{-1} biosorbent dosage. Thus, from an economical point of view, 2.0 mg.L-1 can be selected as an optimum bisorbent dosage for this system.

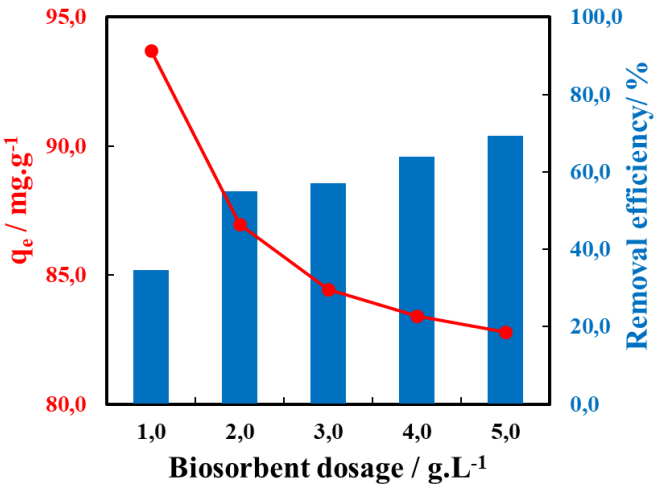

Figure 5. Effects of biosorbent dosage (g.L^{-1}) on uptake of As(V)(initial pH=6.0, C_o=100 mg.L^{-1}, t=120 min)

3.4. Artificial Neural Network Modeling

The three-layer ANN model was used for modeling the biosorption of As(V) onto GPC. The as-obtained experimental data at different operating conditions (Table 1) were applied to train and validate the developed ANN model. The Levenberg-Marquardt algorithm with 100 iterations, "tansig" transfer function for the hidden layer, and a "purelin" transfer function at the output layer were used in the ANN model. The optimal number of hidden neurons was evaluated by the maximization of the coefficient of determination and minimizing MSE of the testing data set (Figure 6.) The results proved that the performance of ANN is depended on the number of neurons in the hidden layer (Table 3). As can be seen from Figure 6., there was a sharp decrease in MSE was detected with an increase in the number of neurons in the hidden layer. The minimum MSE value was calculated to be 0.0014 whereas the maximum R^2 was obtained as 0.9858 by using 12 hidden neurons. Hence, the ANN model containing the hidden layer with 12 neurons was selected as the optimum model for forecasting of biosorption behavior of As(V) onto GPC, and this was used for further analysis.

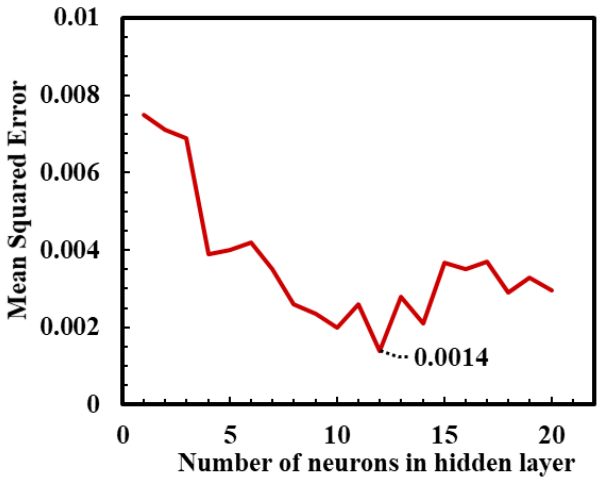

Figure 6. The relation between the MSE and number of neurons in the hidden layer of the developed ANN model

Table 3. The analogy of 20 neurons in the hidden layer for removal efficiency by the ANN model developed with the Levenberg–Marquardt algorithm.

Number of Neurons	MSE	R^2	Number of Neurons	MSE	R^2
1	0.0075	0.8444	11	0.0026	0.9446
2	0.0071	0.8526	12	0.0014	0.9858
3	0.0069	0.8573	13	0.0028	0.9357
4	0.0039	0.9183	14	0.0021	0.9243
5	0.0040	0.9115	15	0.0037	0.9165
6	0.0042	0.9116	16	0.0035	0.9105
7	0.0035	0.9277	17	0.0037	0.9106
8	0.0026	0.9525	18	0.0029	0.9405
9	0.0023	0.9467	19	0.0033	0.9117
10	0.0020	0.9594	20	0.0030	0.9395

Figure 7a. represented the mean squared error values versus the number of epochs for the optimized ANN model. It was observed that after almost 140 epochs the MSE was not changed significantly, so the training was stopped. Figure 7b. presented a comparsion between the experimental and ANN-driven predicted values of the normalized output variable for As(V) biosorption on GPC at the optimum operating conditions. The results confirmed that the developed model is quite satisfactory.

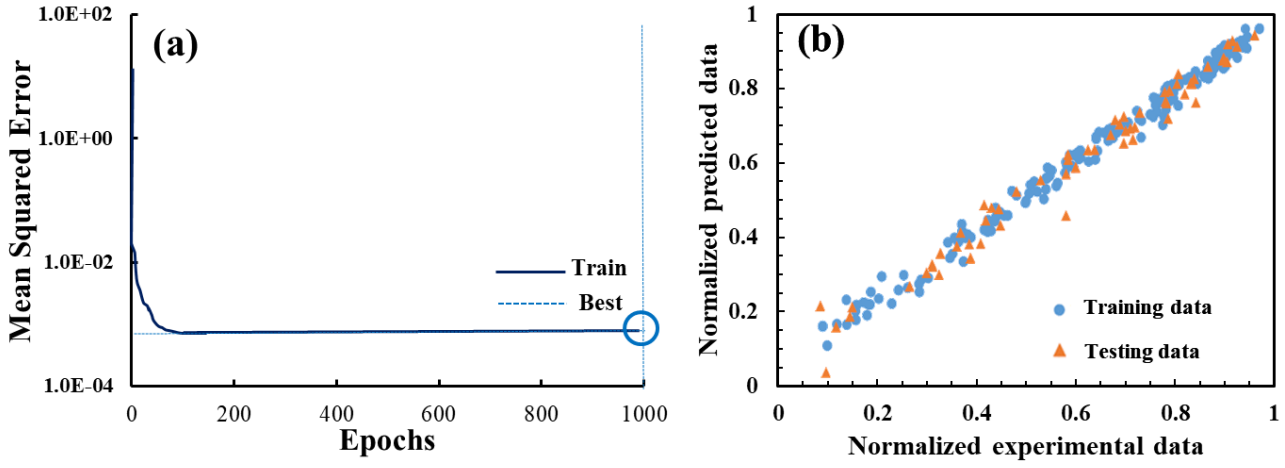

Figure 7. (a) MSE versus the number of epochs (b) the normalized experimental data versus the normalized predicted data

4. Conclusions

Herein, the graphene-like porous carbon with high specific surface area and pore volume was produced from waste orange peel via an eco-friendly, low-cost production pathway, and the potential application as biosorbent for As(V) removal was investigated. The batch biosorption studies were conducted to investigate the effect of initial pH, initial arsenate concentration, contact time, and biosorbent dosage on the removal efficiency of the biosorbents. The optimum pH and the biosorbent dosage were found to be 6.0 and 2.0 $g.L^{-1}$, respectively. It was observed that ca. > 88% of As(V) could be successfully removed from aqueous solution. Furthermore, the biosorption performance of graphene-like porous carbon was forecasted by applying a three-layer ANN with 12 neurons in the hidden layer, using the Levengberg-Marquardt backpropagation algorithm. The outputs of the developed model were in accordance with the experimental values. The results obtained from the ANN model revealed that the values of R^2 and MSE were calculated to be 0.9858 and 0.0014, respectively. The results confirmed that the as-prepared GPC could be applied as a low-cost agricultural waste driven biosorbent as an alternative to commercially available adsorbents for the removal of As(V) from water/wastewater. Moreover, it was concluded that the developed ANN model could be utilized in future studies to optimize and to enhance the removal efficiency of effluents by biosorption under different operating conditions.

References

Abid, M., Niazi, N. K., Bibi, I., Farooqi, A., Ok, Y. S., Kunhikrishnan, A., ... & Arshad, M. (2016). Arsenic (V) biosorption by charred orange peel in aqueous environments. *International journal of phytoremediation*, *18*(5), 442-449.

Aghav, R. M., Kumar, S., & Mukherjee, S. N. (2011). Artificial neural network modeling in competitive adsorption of phenol and resorcinol from water environment using some carbonaceous adsorbents. *Journal of hazardous materials*, *188*(1-3), 67-77.

Almasri, D. A., Rhadfi, T., Atieh, M. A., McKay, G., & Ahzi, S. (2018). High performance hydroxyiron modified montmorillonite nanoclay adsorbent for arsenite removal. *Chemical engineering journal*, *335*, 1-12.

Asfaram, A., Ghaedi, M., Azqhandi, M. A., Goudarzi, A., & Dastkhoon, M. (2016). Statistical experimental design, least squares-support vector machine (LS-SVM) and artificial neural network (ANN) methods for modeling the facilitated adsorption of methylene blue dye. *RSC advances*, *6*(46), 40502-40516.

Beale, M. H., Hagan, M. T., & Demuth, H. B. (2012). Neural network toolbox™ user's guide. In *R2012a, The MathWorks, Inc., 3 Apple Hill Drive Natick, MA 01760-2098, www. mathworks. com*.

Chandana, L., Krushnamurty, K., Suryakala, D., & Subrahmanyam, C. H. (2020). Low-cost adsorbent derived from the coconut shell for the removal of hexavalent chromium from aqueous medium. *Materials Today: Proceedings*, *26*, 44-51.

Chattopadhyay, A., Singh, A. P., Singh, S. K., Barman, A., Patra, A., Mondal, B. P., & Banerjee, K. (2020). Spatial variability of arsenic in Indo-Gangetic basin of Varanasi and its cancer risk assessment. *Chemosphere*, *238*, 124623.

Chow, H., Chen, H., Ng, T., Myrdal, P., & Yalkowsky, S. H. (1995). Using backpropagation networks for the estimation of aqueous activity coefficients of aromatic organic compounds. *Journal of chemical information and computer sciences*, *35*(4), 723-728.

Çelebi, H. (2020). Recovery of detox tea wastes: Usage as a lignocellulosic adsorbent in Cr6+ adsorption. *Journal of Environmental Chemical Engineering*, 104310.

Das, S. K., Das, A. R., & Guha, A. K. (2007). A study on the adsorption mechanism of mercury on Aspergillus versicolor biomass. *Environmental science & technology*, *41*(24), 8281-8287.

Dutta, S., Parsons, S. A., Bhattacharjee, C., Bandhyopadhyay, S., & Datta, S. (2010). Development of an artificial neural network model for adsorption and photocatalysis of reactive dye on TiO2 surface. *Expert Systems with Applications*, *37*(12), 8634-8638.

Ebrahimi, B., Mohammadiazar, S., & Ardalan, S. (2019). New modified carbon based solid phase extraction sorbent prepared from wild cherry stone as natural raw material for the pre-concentration and determination of trace amounts of copper in food samples. *Microchemical Journal*, *147*, 666-673.

Elemen, S., Kumbasar, E. P. A., & Yapar, S. (2012). Modeling the adsorption of textile dye on organoclay using an artificial neural network. *Dyes and Pigments*, *95*(1), 102-111.

Fawzy, M., Nasr, M., Nagy, H., & Helmi, S. (2018). Artificial intelligence and regression analysis for Cd (II) ion biosorption from aqueous solution by Gossypium barbadense waste. *Environmental Science and Pollution Research*, *25*(6), 5875-5888.

Ghaedi, M., Hosaininia, R., Ghaedi, A. M., Vafaei, A., & Taghizadeh, F. (2014a). Adaptive neuro-fuzzy inference system model for adsorption of 1, 3, 4-thiadiazole-2, 5-dithiol onto gold nanoparticales-activated carbon. *Spectrochimica Acta Part A: Molecular and Biomolecular Spectroscopy*, *131*, 606-614.

Ghaedi, M., Ghaedi, A. M., Abdi, F., Roosta, M., Sahraei, R., & Daneshfar, A. (2014b). Principal component analysis-artificial neural network and genetic algorithm optimization for removal of reactive orange 12 by copper sulfide nanoparticles-activated carbon. *Journal of Industrial and Engineering Chemistry*, *20*(3), 787-795.

Guo, Y., Tan, C., Sun, J., Li, W., Zhang, J., & Zhao, C. (2020). Porous activated carbons derived from waste sugarcane bagasse for CO2 adsorption. *Chemical Engineering Journal*, *381*, 122736.

He, C., Lin, H., Dai, L., Qiu, R., Tang, Y., Wang, Y., ... & Ok, Y. S. (2020). Waste shrimp shell-derived hydrochar as an emergent material for methyl orange removal in aqueous solutions. *Environment international*, *134*, 105340.

Irem, S., Islam, E., Mahmood Khan, Q., Anwar ul Haq, M., & Jamal Hashmat, A. (2017). Adsorption of arsenic from drinking water using natural orange waste: kinetics and fluidized bed column studies. *Water Science and Technology: Water Supply*, *17*(4), 1149-1159.

Khaskheli, M. I., Memon, S. Q., Siyal, A. N., & Khuhawar, M. Y. (2011). Use of orange peel waste for arsenic remediation of drinking water. *Waste and Biomass Valorization*, *2*(4), 423.

Karaman, C., Aktas, Z., Bayram, E., Karaman, O., & Kızıl, Ç. (2020). Correlation Between the Molecular Structure of Reducing Agent and pH of Graphene Oxide Dispersion On the Formation of 3D-Graphene Networks. *ECS Journal of Solid State Science and Technology*.

Kodal, Süheyla Pınar, and Zümriye Aksu. "Cationic surfactant-modified biosorption of anionic dyes by dried Rhizopus arrhizus." *Environmental technology* 38, no. 20 (2017): 2551-2561.

Liang, S., Guo, X., Feng, N., & Tian, Q. (2009). Application of orange peel xanthate for the adsorption of Pb2+ from aqueous solutions. *Journal of Hazardous Materials*, *170*(1), 425-429.

Lu, D., Cao, Q., Li, X., Cao, X., Luo, F., & Shao, W. (2009). Kinetics and equilibrium of Cu (II) adsorption onto chemically modified orange peel cellulose biosorbents. *Hydrometallurgy*, *95*(1-2), 145-152.

Ma, J., Li, T., Liu, Y., Cai, T., Wei, Y., Dong, W., & Chen, H. (2019). Rice husk derived double network hydrogel as efficient adsorbent for Pb (II), Cu (II) and Cd (II) removal in individual and multicomponent systems. *Bioresource technology*, *290*, 121793.

Meng, Q., Qin, K., Ma, L., He, C., Liu, E., He, F., ... & Zhao, N. (2017). N-doped porous carbon nanofibers/porous silver network hybrid for high-rate supercapacitor electrode. *ACS applied materials & interfaces*, *9*(36), 30832-30839.

Molga, E. J., & Westerterp, K. R. (1997). Neural network based model of the kinetics of catalytic hydrogenation reactions. In *Studies in Surface Science and Catalysis* (Vol. 109, pp. 379-388). Elsevier.

Mustafa, Y. A., Jaid, G. M., Alwared, A. I., & Ebrahim, M. (2014). The use of artificial neural network (ANN) for the prediction and simulation of oil degradation in wastewater by AOP. *Environmental Science and Pollution Research*, *21*(12), 7530-7537.

Naik, A. D., & Bhagwat, S. S. (2005). Optimization of an artificial neural network for modeling protein solubility. Journal of Chemical & Engineering Data, 50(2), 460-467.

Nia, R. H., Ghaedi, M., & Ghaedi, A. M. (2014). Modeling of reactive orange 12 (RO 12) adsorption onto gold nanoparticle-activated carbon using artificial neural network optimization based on an imperialist competitive algorithm. *Journal of Molecular Liquids*, *195*, 219-229.

Omwene, P. I., Çelen, M., Öncel, M. S., & Kobya, M. (2019). Arsenic removal from naturally arsenic contaminated ground water by packed-bed electrocoagulator using Al and Fe scrap anodes. Process Safety and Environmental Protection, 121, 20-31.

Pathak, P. D., Mandavgane, S. A., & Kulkarni, B. D. (2016). Characterizing fruit and vegetable peels as bioadsorbents. Current Science, 2114-2123.

Rahaman, M. S., Basu, A., & Islam, M. R. (2008). The removal of As (III) and As (V) from aqueous solutions by waste materials. Bioresource technology, 99(8), 2815-2823.

Rozman, U., Kalčíková, G., Marolt, G., Skalar, T., & Gotvajn, A. Ž. (2020). Potential of waste fungal biomass for lead and cadmium removal: Characterization, biosorption kinetic and isotherm studies. *Environmental Technology & Innovation*, 100742.

Su, T., Guan, X., Tang, Y., Gu, G., & Wang, J. (2010). Predicting competitive adsorption behavior of major toxic anionic elements onto activated alumina: A speciation-based approach. *Journal of hazardous materials*, *176*(1-3), 466-472.

Tran, T. H., Le, A. H., Pham, T. H., Nguyen, D. T., Chang, S. W., Chung, W. J., & Nguyen, D. D. (2020). Adsorption isotherms and kinetic modeling of methylene blue dye onto a carbonaceous hydrochar adsorbent derived from coffee husk waste. *Science of The Total Environment*, *725*, 138325.

World Health Organization (WHO). (2011). Guidelines for drinking-water quality. *WHO chronicle*, *38*(4), pp 186.